Screening and Design of Aqueous Zinc Battery Electrolytes Based on the Multimodal Optimization of Molecular Simulation

Wei Feng,[†] Luyan Zhang,[†] Yaobo Cheng,[‡] Jin Wu,[‡] Chunguang Wei,[‡] Junwei Zhang,[‡] and Kuang Yu*[,†]

†*Tsinghua Shenzhen International Graduate School, Shenzhen 518055, Guangdong, P. R. China*

‡*Shenzhen Cubic-Science Co., Ltd.*

E-mail: yu.kuang@sz.tsinghua.edu.cn

Abstract

Aqueous batteries, such as aqueous zinc-ion batteries (AZIB), have garnered significant attention because of their advantages in intrinsic safety, low cost, and eco-friendliness. However, aqueous electrolytes tend to freeze at low temperatures, which limits their potential industrial applications. Thus, one of the core challenges in aqueous electrolyte design is optimizing the formula to prevent freezing while maintaining good ion conductivity. However, the experimental trial-and-error approach is inefficient for this purpose, and existing simulation tools are either inaccurate or too expensive for high-throughput phase transition predictions. In this work, we employ a small amount of experimental data and differentiable simulation techniques to develop a multimodal optimization workflow. With minimal human intervention, this workflow significantly

[1]Wei Feng and Luyan Zhang contributed equally to this work.

enhances the prediction power of classical force fields for electrical conductivity. Most importantly, simulated electrical conductivity can serve as an effective predictor of electrolyte freezing at low temperatures. Generally, the workflow developed in this work introduces a new paradigm for electrolyte design. This paradigm leverages both easily measurable experimental data and fast simulation techniques to predict properties that are challenging to access using either approach alone.

1. Introduction

Battery technology is the cornerstone of many industrial sectors, including electric vehicles and various portable electronics in our daily life. The electrolyte, as a crucial part of battery, plays a significant role in determining battery performance. Thus, a comprehensive understanding of electrolyte structures and properties is necessary for the future development of next-generation battery technology.

Electrolytes typically consist of salts, solvents, and additives. The salts provide ions for charge transport, and solvents provide the basic solvation environment, while additives are used to further fine-tune the electrolyte properties. To obtain better electrolytes, one can either change the molecular structures or fine-tune the composition ratio of all components, leading to a gigantic design space. Formula optimization based on trial-and-error and human intuition can be very inefficient, so systematic screening is often necessary, which is, however, still a quite challenging task. Currently, both experimental and simulation approaches can be used for high-throughput screening.[1–3] Experimental approaches (especially in vivo tests) are reliable but can be economically expensive and time consuming on a large scale. More importantly, macroscopic experimental tests do not provide detailed microscopic structural and dynamic information. This information is needed to understand the structure-property relationship, which is necessary for the rational design of electrolytes.[4,5] In contrast, computational tools such as molecular dynamics (MD) are more cost-effective and informative on the atomic scale. However, MD simulation is haunted by inaccurate force fields (FF)

and sampling problems, rendering its prediction untrustworthy. Moreover, MD simulation is largely limited to predicting basic homogeneous bulk physical properties. However, complex phenomena such as interfacial chemistry and phase transitions involving large time and spatial scales have profound impacts on battery performance. Simulating these phenomena directly using MD is extremely non-trivial and is still nearly impossible to do in high-throughput. To solve these problems and gain a more comprehensive understanding, both experimental and computational tools need to be combined.

In this work, we focus on the screening of aqueous zinc ion battery (AZIB) electrolytes, which is a typical problem as stated above. AZIB is gaining popularity because of its low cost and non-flammability.[6–8] Aqueous electrolytes also exhibit ionic conductivity one to two orders of magnitude higher than organic electrolytes, making them a promising alternative energy storage technology.[9,10] However, compared to commercial organic electrolytes, which is a relatively more mature technology, AZIB still suffers from a number of problems, such as the stability of electrode materials[11] and the modulation of solid electrolyte interphases (SEI).[12,13] One of the key issues in AZIB is that aqueous electrolytes are easy to freeze, deteriorating battery performance at low temperatures. Consequently, it is necessary to optimize organic additives and salt concentrations to prevent freezing and increase conductivity at low temperatures,[14–17] complicating the design of the electrolyte formula. As stated above, high-throughput virtual screening based on MD simulation can be helpful in electrolyte design, but is currently hindered by two major difficulties:

1. An accurate and efficient potential energy surface (PES) suitable for large-scale virtual screening is still missing. The most reliable PES would be the ab initio (mostly based on density functional theory, DFT) PES, leading to the so-called AIMD (ab initio MD) approach. But its computational cost is too high to be practical for virtual screening. Another alternative option is machine learning MD (MLMD), which learns a ML PES from a large number of ab initio data.[18–22] MLMD is relatively faster compared to AIMD while retaining its accuracy, but the current ML PES does not possess the transferability needed for

formula screening. There are large models such as BAMBOO[22] and MACE-OFF23,[23] aimed at training a general electrolyte ML PES. But such efforts still only exist for commercial organic electrolytes, with compromised accuracy and limited chemical space coverage. Other hybrid approaches such as PhyNEO[24] need ab initio many-body data for training, which is also too expensive for the screening of aqueous electrolytes. Due to these reasons, the main workhorse in this area is still the classical fixed point charge FF,[25–30] the main advantage of which is the exceptional simulation speed. With carefully fine-tuned parameters, the classical FF can be accurate enough for the purpose of large-scale screening, but the parameter optimization process is highly non-trivial. As we will show in this work, the off-the-shelf FF can be qualitatively insufficient for any screening tasks.

2. Even with the fast classical FF, it is still difficult for MD to directly simulate the freezing process. The freezing of pure water has been systematically studied using MD for more than two decades, while still being an extremely challenging problem.[31] High-throughput simulation of the freezing processes of complex aqueous electrolytes would be nearly impractical. So far, a theoretical tool for predicting electrolyte freezing still does not exist, whereas such a tool is indispensable to improve the low-temperature performance of AZIB.

In response to these challenges, in this work we aim to develop a systematic workflow that combines both experimental and computational methods to perform accurate prediction and virtual screening for AZIB electrolytes. Following common practice in the development of classical FF, easily measurable experimental data such as densities and evaporation enthalpies are used to generate classical FF that are specifically tailored for aqueous electrolyte systems.[32–34] However, unlike conventional hand-crafted parameter tweaking, multimodal top-down optimization is conducted using the advanced automatic differentiable (AD) MD (ADMD) technique.[35–38] This new technique allows us to optimize FF automatically without any human intervention. ADMD transforms top-down FF fine-tuning from a highly specialized, tedious, and time-consuming task into a task that can be conducted automati-

cally and efficiently. This enables us to use any available experimental data to update the FF on a routine basis, which is important for the systematic exploration of the electrolyte design space. The optimized FF is then used to screen the AZIB electrolyte formulae, targeting the electrical conductivity (especially at low temperatures) as the main property to optimize. In comparison with the experimental data, we further find that the ionic conductivity predicted using optimized FF is an excellent predictor for the freezing of electrolytes. By combining easily measurable experimental data and fast MD simulation, we essentially enables the screening of the low-temperature performance of AZIB electrolytes, which was hard to probe directly using either approach alone.

2. Model and Methodology

2.1 AZIB Electrolyte Screening

As mentioned above, AZIB electrolytes have garnered significant industrial attention because of their low cost, non-flammability, and high conductivity. In this study, we focus on a specific AZIB electrolyte system primarily composed of zinc sulfate, with minor amounts of manganese sulfate and polyol-based organic additives such as ethylene glycol (EG) and glycerol (GI). For this system, we first prepared a small set of formulations and measured their densities and conductivities at various temperatures, thus establishing a preliminary experimental database for subsequent FF training, validation, and simulation prediction. These experimental data encompass electrolyte densities and conductivities for varying concentrations (from 1 M to 2.5 M) of $ZnSO_4$ and $MnSO_4$, different proportions (0 to 30 wt. %) of organic additives EG and GI, at various temperatures (253 K, 273 K, 298 K, 333 K), totaling about 140 data points. We selected approximately half of them for the training of FF and half as testing set. All data are available in supplementary information.

In the selection process, we adhered to the principle of evenly choosing points across different temperature ranges, ion concentration ranges, and organic additive concentration

ranges to enhance the coverage of the training and testing data in the formulation space. In addition, note that we always leave the points with the best and worst performances within each range outside of the training set. Therefore, the prediction of these points in the testing stage would be an extrapolation, instead of an interpolation in the design space. This approach validates the capability of our model to identify the best and worst performers outside of the training range, and this capability is crucial for formula screening.

We further note that this experimental database particularly emphasizes the performance of these formulations at different temperatures to explore the temperature-dependence of their properties, especially at low temperatures (253 K). At such conditions, aqueous electrolytes face the risk of freezing, accompanied by a substantial reduction in conductivity. Based on this database, our aim was to train theoretical models applicable across a broad temperature range, validate their accuracies, and use them to identify AZIB electrolyte formulations that maintain good conductivity at low temperatures or are at risk of freezing.

To achieve this screening, the primary challenge lies in efficiently utilizing the limited experimental data to generate accurate theoretical models, conduct high-throughput simulations at low cost, and identify target formulations for further experimental iteration. We need to utilize small amount of experimental data to develop a generally applicable simulation approach.

2.2 Workflow

In this work, we developed an AZIB electrolyte screening workflow that integrates both experimental data and theoretical tools, utilizing fast and cost-effective classical MD simulations. As shown in Figure 1, our workflow starts with a small amount of experimental data and uses them to systematically refine the classical fixed point charge FF based on multimodal optimization. The optimization results in a significantly better prediction for thermodynamic and transport properties across different formulations and temperature ranges. In addition, we used refined FF to screen different formulations of aqueous electrolytes, expand-

ing the electrolyte space, and then found the target formulations at low temperatures and experimentally verified their performance. In principle, multiple iterations can be conducted to achieve a robust and sustainable cycle, in which experimental data enhance theoretical simulations, and theoretical simulations guide further experiments in turn.

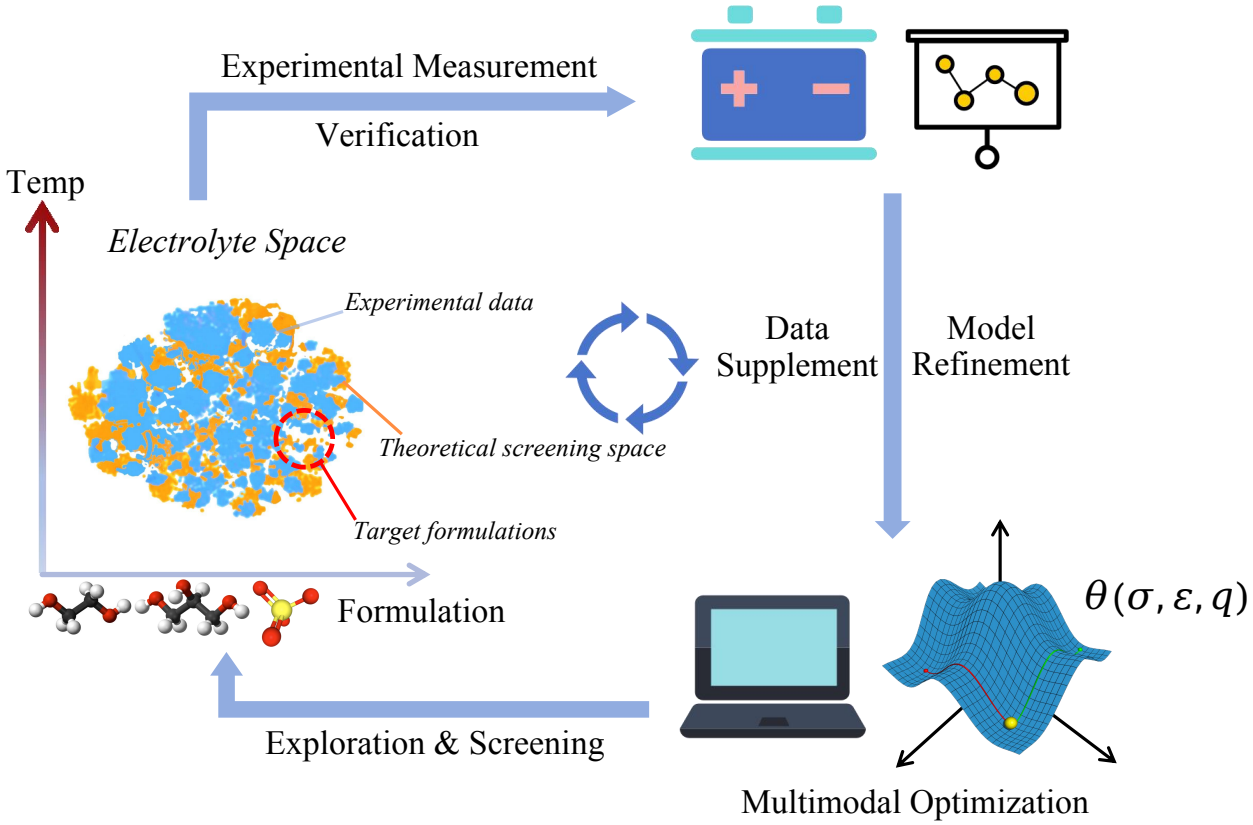

Figure 1: The workflow of integrating experiments and simulation for screening of AZIB electrolytes.

The basic idea of our workflow is to use experimental data to realign the FF used in MD simulation. Tailoring FF parameters for specific application is an old idea and has been done in numerous previous works.[39–43] However, these works are conducted primarily on simple systems with a limited number of adjustable parameters. For complex multicomponent systems with large number of parameters and constantly cumulating experimental data (e.g., electrolytes), the fine-tuning of FF should be performed routinely in a scalable, automatic, and reproducible fashion. ADMD simulation provides an efficient approach to carry out such a task. In this work, we use the reweighting MBAR approach implemented in our previous

work[38] to optimize the FF parameter. Easily accessible data including the evaporation enthalpies of organic additives and densities of the electrolytes at various compositions and temperatures are combined as our fitting target. Conductivities are used mainly for charge scaling realignment and validation purposes. This multimodal optimization transforms the training of the FF from years of expert handcrafting into a simple two-week process without human supervision, which is necessary to keep up with the update of the experimental data.

2.2.1 Theoretical Model

In this work, we used GAFF (General Amber Force Field), commonly used in organic molecules and drug molecular systems,[27–29] as our initial guess for the salt and organic additive parameters. SPC/E model[44] was always used for water without optimization. In the optimization, we only modified the nonbonded interactions (the Lennard-Jones (LJ) and electrostatic charges), which essentially dominates the conducting behavior of the electrolyte.

The two LJ parameters (σ and ϵ) are sensitive to different data: σ has a greater influence on density,[45,46] while the evaporation enthalpy is in a closer connection with ϵ.[47,48] Therefore, both the densities and evaporation enthalpies are used to regularize the LJ parameters in ADMD simulation. To improve the generality of the model, we use degenerate parameters, a common strategy in FF fitting[49] which can enhance parameter transferability between different molecules (see Section 3 in SI).

In addition to the LJ parameters, an adjustable scaling factor was applied on all atomic charges, which has a critical effect on electrical conductivity. Charge-scaled models and polarizable FF have both been proven to be effective in predicting transport properties,[50,51] but polarizable model is computationally more intensive, compromising the efficiency of MD and its applicability in large-scale screening. So we focused on the charge-scaled model with different scaling factors to obtain an effective charge that can describe the charge shielding effect in electrolytes. Although it is a common approach in previous studies, it has been a challenge for charge-scaled models to simultaneously achieve accurate predictions for both

thermodynamic and transport properties.[51–53] To solve this problem, the LJ parameters were fine-tuned against density and evaporation enthalpy data under different scaling factors, while the charge scaling factor was manually scanned to achieve the best accuracy for electrical conductivity. As we show below, such a strategy reaches a much better balance between the prediction capabilities of different properties.

2.2.2 Multimodal Optimization

To realize multimodal optimization, we used the Differentiable Molecular Force Field (DMFF)[38] program to perform trajectory reweighting,[54] which avoids expensive backpropagation through MD trajectory. During the optimization, we targeted a large number of systems at different temperatures and formulations simultaneously. We constructed an objective function encompassing multiple properties to obtain parameters suitable for various systems.

Specifically, the loss function is constructed as following:

$$\text{Loss} = \sum_{T,s} \omega_T (\rho - \rho_{\text{ref}})^2 + (\Delta H^{\text{EG}} - \Delta H^{\text{EG}}_{\text{ref}})^2 \tag{1}$$

where ρ is the simulated electrolyte density and ρ_{ref} is the experimental data, the same as for ΔH. In this work, we study two organic additives: EG and GI. Since these two organic molecules share FF parameters, to examine the transferability of our parameters in different molecules, we only included ΔH^{EG} in our object function, while leaving GI as our testing examples. The reference value of $\Delta H^{\text{EG}}_{\text{ref}}$ was taken from the CRC database[55] and fixed at 298 K during the optimization. In the loss function, ω_T represents a temperature-dependent weighting factor, which is introduced because the number of experimental data points varies between different temperatures in the training dataset. ω_T was taken to ensure equal contributions from data points in different temperatures, warranting balanced performance of the model in a wide temperature range.

In practice, we first optimized the density to achieve a relatively accurate level, then

both density and evaporation enthalpy data are employed to finish the final refinement. In the final refinement stage, two ADAM optimizers were initialized separately, each using either density or enthalpy gradients to update. The parameter updates from both optimizers are used alternately during the optimization. In our experience, this strategy ensures that different physical data with different magnitudes do not interfere with each other in gradient updates. Moreover, arbitrary relative weights can be avoided between different experimental data types.

2.2.3 Computational Details

Robust and standard calculation procedures for properties (i.e., density, evaporation enthalpy, and electrical conductivity) are essential in our workflow. Densities were directly derived from NPT simulations, while evaporation enthalpies were evaluated using the averaged potential energies in gas and liquid phases (i.e., V_{gas} and V_{liquid}), as shown in the following equation:[56]

$$\Delta H = V_{\text{gas}} - V_{\text{liquid}} + RT \tag{2}$$

The situation for electrical conductivity is slightly more complicated as multiple methods exist to compute electrical conductivity in electrolyte. In previous studies, one often first determines the self-diffusion coefficient from the mean square displacement (MSD), then use the Nernst-Einstein relationship to obtain the conductivity.[57,58] This approach is not rigorous because the Nernst-Einstein equation is only applicable to ideal dilute solutions, when the correlation between the diffusion of positive and negative ions can be neglected.[59] Although more accurate methods exist (such as the mutual diffusion coefficient method[60–62]), but they have relatively poorer convergence in our systems.[59,63,64] Therefore, we choose to calculate the conductivity by directly integrating the current time correlation function

(TCF).[47,65] The instantaneous ionic current is computed as:

$$\mathbf{J}(t) = \sum_i q_i \mathbf{v}_i \tag{3}$$

where q_i and v_i are the charges and velocities of ions. The TCF then can be computed using moving average along sampled trajectories:

$$C_J(\tau) = \langle \mathbf{J}(t) \cdot \mathbf{J}(t+\tau) \rangle \tag{4}$$

Then the conductivity can be obtained by integrating TCF:

$$\sigma = \frac{1}{k_B T V} \int_0^\infty C_J(\tau)\, d\tau \tag{5}$$

More details of simulations and MD settings are inlcuded in Supplementary Information.

Initial GAFF parameters were obtained using Ambertools,[66,67] and the initial structures in different compositions were constructed using Packmol.[68] All non-differentiable simulations were conducted using OpenMM.[69,70] The entire optimization process was conducted on a single V100 card, undergoing over 60 iterations and taking approximately 10 days to complete. All procedures were fully automated, requiring no manual intervention.

3. Results and Discussion

3.1 Performance of Optimized Model

Following the aforementioned AZIB electrolyte screening workflow, we performed multiple rounds of multimodal optimization, refining the LJ parameters under charge-scaled models with different scaling factors (0.6, 0.7, and 0.8). We then compared the original model (GAFF + SPC/E), the charge-scaled model (one of the most commonly used approaches in previous literature[71,72]), and the corresponding optimized models generated in this work.

The results are reported in Figure 3 and Figure S2. As shown in Figure S2, without system-specific optimization, the original GAFF model generates significant outliers in density, and the predicted conductivities show essentially no correlation with experimental results. This performance clearly illustrates the deficiency of universal FF in electrolyte screening, and MD simulations using such a FF can be seriously misleading. For comparison, the charge-scaled model performs much more robustly in conductivity predictions when the right scaling factor is used. However, since charge parameterization is strongly coupled with LJ parameters, adjusting charges alone significantly deteriorates the model performance in densities (Figure S2) and evaporation enthalpies (Table 1). In Figure 2, we show the trends of density and conductivity errors during the density optimization cycles starting from the charge-scaled models. For all charge scaling factors, by optimizing density, the electrical conductivity error is also reduced. This shows how the learned parameters can be transferred in the predictions of different properties. We find that the inclusion of EG evaporation enthalpy in the fitting target worsens the accuracy of conductivity. This shows the balance between dynamic and thermodynamic properties, which is an inherent limitation originating from the inaccurate function form used in the classical FF. Nevertheless, compared to the charge-scaled model, the final optimized model still shows better performance in electrical conductivity, regardless of the scaling factor. In addition, the predictions of the density and evaporation enthalpy are also significantly more accurate (see Figure S2 and Table 1). We also note that the improvement achieved in the EG evaporation enthalpy is also observed for GI, which was not included in the fitting target, proving the excellent chemical transferability of the optimized model (see Table 1). Therefore, we conclude that the automatically optimized FF reaches a much better performance compared to both initial GAFF and charge-scaled GAFF (regardless of the value of the scaling factor) and thus will be used in all subsequent studies.

To finalize the FF model for formula screening, we still need to determine the optimal value for the charge scaling factor. Using conductivity errors as our gauge, the scaling factor is set to 0.7 at 273 K and 298 K. However, at low temperature (253 K), 0.6 gives a better

result, while 0.8 is optimal at higher temperature (333 K). We plotted the heat map of the correlation between scaling factors and temperatures in Figure S3. This is physically understandable, as the charge shielding effect weakens at higher temperatures, so the scaling factor should be larger when the temperature increases. The final results for the training set are plotted in Figure 3a and b, computed using the temperature-dependent charge scaling factors and in comparison with the original and the corresponding charge-scaled GAFF. It is clear that multimodal optimization based on small amount of experimental data largely enhances the accuracy of MD. We further examine the optimized model in the extrapolation test dataset, which is composed by the worst and the best performers at each temperature. The results are plotted in Figure 3c and d. Once again, the strong predictive power of the optimized model is clearly demonstrated, in comparison with the original GAFF.

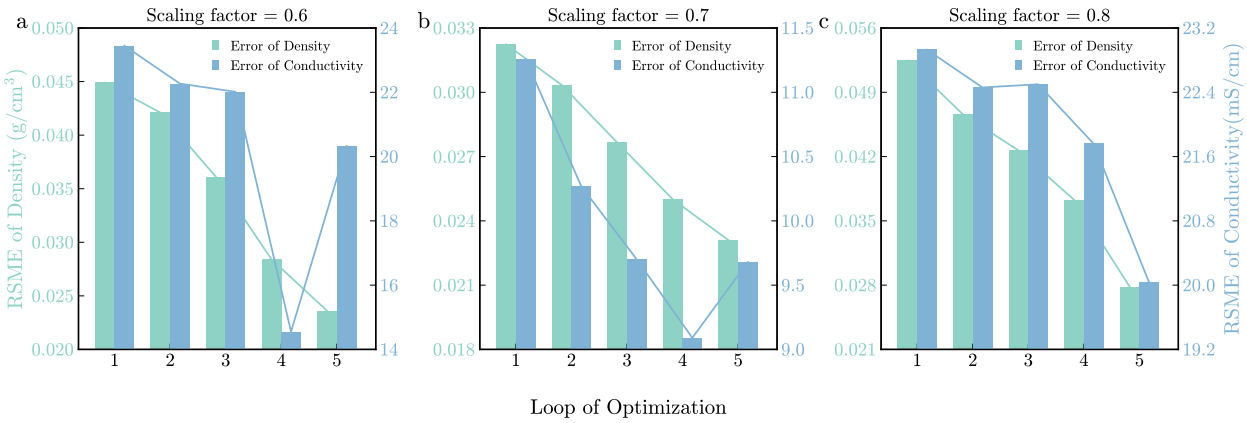

Figure 2: The trends of density and conductivity errors during the optimization: (a), (b), and (c) respectively show the changes under different scaling factors.

Table 1: Prediction errors of thermodynamic quantities for different models

	Initial	Only CS(0.6)	Opt(0.6)	Only CS(0.7)	Opt(0.7)	Only CS(0.8)	Opt(0.8)
density	13.78%	4.49%	2.82%	3.22%	2.71%	5.24%	2.91%
ΔH (EG)	7.85%	52.59%	35.14%	41.69%	25.92%	31.81%	18.45%
ΔH (GI)	20.69%	49.56%	31.76%	43.33%	30.99%	35.34%	23.08%

To investigate the reliability of the model in greater details, we further examine its capability to capture the quantitative trends of electrical conductivity with respect to tem-

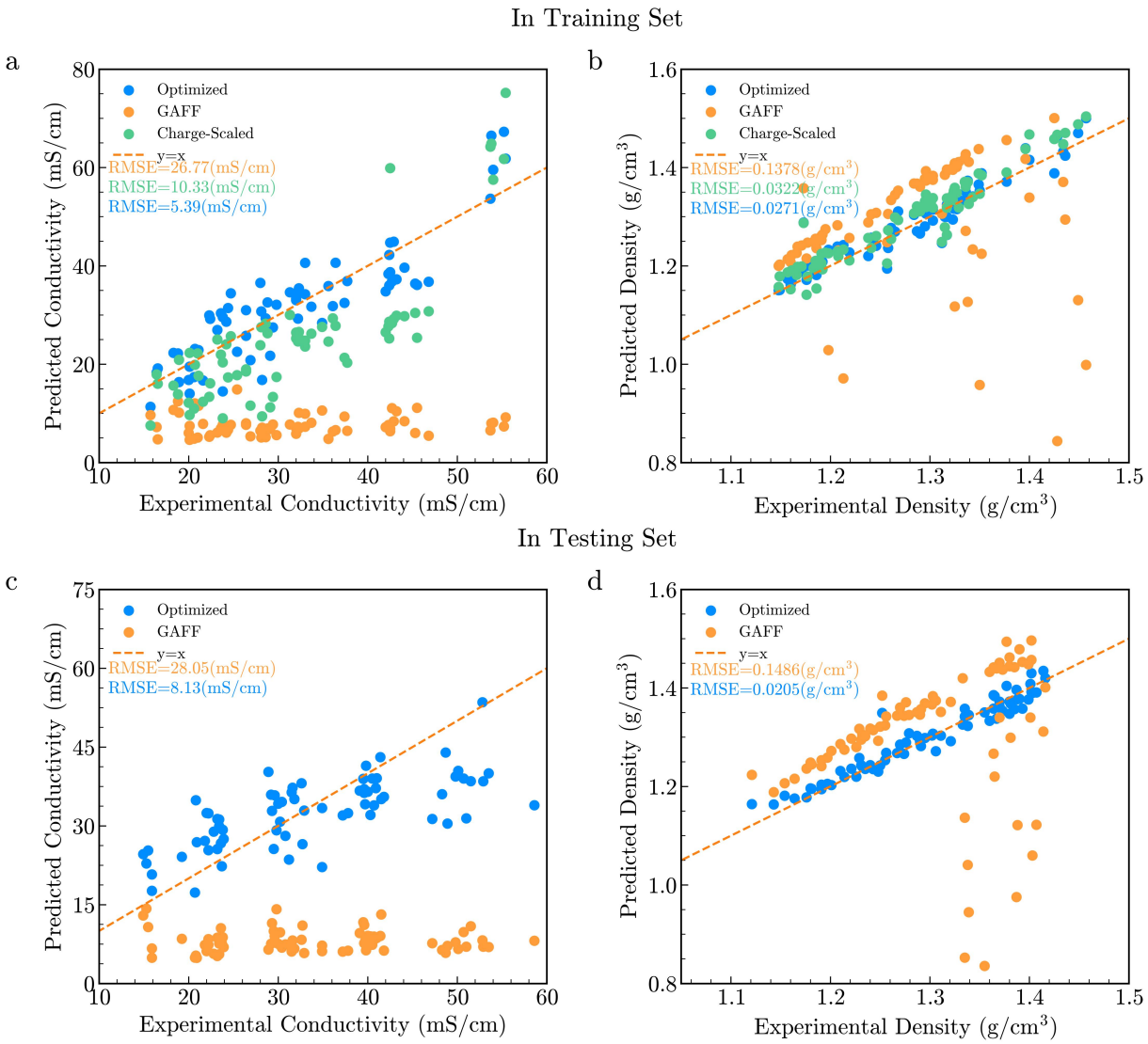

Figure 3: Final performance of different models in training and testing sets : (a)(b) respectively show the prediction results of conductivity and density of optimized model in the training set, in comparison with GAFF and charge-scaled model; (c)(d) show the prediction results of optimized model in the testing set, in comparison with GAFF.

peratures and composition ratios. Capturing such trends is important for the physical understanding of the electrolyte behavior, thus is crucial for the rational design of electrolytes. As illustrated in Figure 4a, we systematically increase EG concentration in the 1.5 M $ZnSO_4$ + 0.1 M $MnSO_4$ solution. A high concentration of organic additive is typically beneficial in preventing freezing at low temperature, but it lowers the electrical conductivity at room temperature (298 K). The effect can be caused by many reasons, including: dilution of ionic concentration due to the non-ionic nature of organic additives, the formation of ion pairs or clusters with the organic compounds that reduce the number of free ions, increased viscosity that hinders ion mobility, and structural changes in the aqueous solution that impedes ion movement.[14–17] Multiple factors contribute to the decrease in conductivity, a trend that both experiments and theoretical simulations have discovered. This effect is clearly observed in Figure 4a, as the predicted conductivity drops from 60 mS / cm to 15 ms / cm by adding 30 wt. % of EG.

Another more interesting example is given in Figure 4b, which shows the temperature dependence of the conductivity for 2 M $ZnSO_4$ + 20 wt. % EG. The conductivity shows a non-monotonic trend with a turning point at 298 K. This complex behavior can be attributed to two competing effects: On the one hand, high temperature leads to enhanced ion mobility and reduced viscosity, which contributes to increasing conductivity; On the other hand, the dielectric constant of water decreases when temperature increases, resulting in increased ion pairing, leaving fewer free ions available for conduction. Different effects may dominate in different temperature ranges, giving the complex non-monotonic temperature dependence. The optimized model accurately captures both the non-monotonic dependence and the position of the turning point at 298 K, highlighting its ability to describe all the relevant underlying physical effects.

In summary, through an automatic multi-modal optimization, we significantly enhance the model's performance in predicting the thermodynamic and transport properties of AZIB electrolytes. It also accurately reflects the physical phenomena of conductivity variations

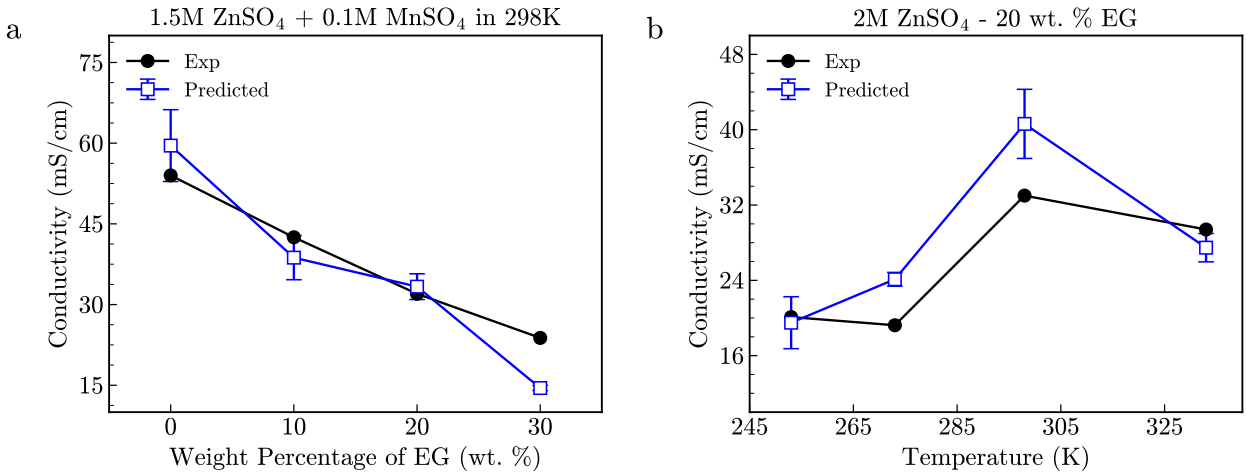

Figure 4: The trends of electrolyte conductivity changes under different conditions: (a) shows the conductivity changes with respect to the weight percentage of organic additive EG. (b) shows the conductivity changes with respect to temperature. Both the predicted values and the experimental measurements are presented in the figure.

under different conditions, which makes it perfectly adequate for formula exploration. As mentioned previously, this optimization and the MD simulation based on classical FF is cost-effective and fully automated, which is crucial for industrial applications.

3.2 Exploring AZIB Electrolytes at Low Temperature

After a comprehensive validation of the model, we further use it to explore the formulation space at low temperatures. Given the limited accuracy of classical MD, it is still difficult to achieve a quantitative prediction of all physical properties. Furthermore, while electrical conductivity is one of the most relevant key properties in electrolyte screening, high conductivity at room temperature alone does not necessarily make it a good electrolyte. As mentioned in the Introduction, a more important issue is that aqueous electrolytes are at risk of freezing,[14–17] which is the main factor preventing their industrial application in low temperature environments. However, freezing behavior is difficult to approach directly using either experimental or simulation methods. Therefore, in this part, our aim is to assess whether the optimized model could accurately distinguish good and bad performers at low temperatures, especially if it can help us identifying freezing failures before experimental

trials.

To explore the electrolyte formulation space, we fix the temperature at 253 K and vary the salt concentration from 1.5M to 2.5M, and the content of organic additives (EG and GI) from 10 wt. % to 40 wt. %. Evenly spaced grid points are used to sample the salt and additive concentrations, resulting in more than 400 formulations. We compute their conductivity using MD and select the three formulations with the highest conductivity for experimental validation. These results are then compared with the top three formulations with best conductivity in the original dataset at 253 K, as shown in Figure 5. As is shown, the conductivity errors of the model in the newly explored best performers (marked by the yellow dots in Figure 5) are comparable or even smaller than the errors of the original best performers (marked by blue dots), again showing the extrapolation capability of the optimized model. The three new best performers feature an experimental conductivity at 253 K of 18.92 mS/cm (1M $ZnSO_4$ + 0.1M $MnSO_4$ with 20 wt. % EG), 16.42 mS/cm (1M $ZnSO_4$ + 0.1M $MnSO_4$ with 30 wt. % EG), and 15.28 mS/cm (2M $ZnSO_4$ + 0.1M $MnSO_4$ with 30 wt. % EG), respectively, which are readily available for more comprehensive battery tests.

More importantly, in the newly explored formulations, we can successfully separate the best and worst performers with high confidence. Specifically, when the predicted conductivity is lower than 10 mS/cm, it always shows an ultra-low experimental conductivity of 0.5 mS/cm, indicating a freezing or vitrification failure (labeled by the blue stars in Figure 5). Therefore, even though simulating the freezing process directly is still a challenging task, we can easily identify and rule out the freezers using low liquid conductivity as an indicator, which can be computed conveniently using fast classical MD. This is physically reasonable because sluggish diffusion dynamics in a liquid is a strong sign of subsequent freezing on a longer time scale. Moreover, it is important to note that this predictive power comes from the carefully fine-tuned theoretical model based on experimental data. To show this, we also compute the conductivities of the three freezers using the normal charge-scaled model, which

are labeled by the red stars in Figure 5. The computed conductivities by the charge-scaled model are reaching 18 mS/cm, which is completely inseparable from the best performers, thus being useless in formula exploration. Therefore, by combining a limited amount of easily measurable experimental data (such as densities and conductivities) and fast MD simulations, we effectively create a highly efficient tool to predict the complex phase-transition at low temperature. Furthermore, this tool is created fully automatically, and can be constantly self-improved using new experimental data and is free from human cherry-picking. In all, we show that with an extremely low cost, our hybrid experimental/computational method serves as an effective approach aiding the discovery of new electrolytes at low temperatures.

4. Conclusion and Outlook

In this work, we developed a comprehensive optimization framework to refine classical FF based on simple experimental measurements, yielding a robust theoretical model for AZIB electrolytes. By recalibrating classical MD using experimental data, we can promote the prediction accuracy to densities and electrical conductivities by orders of magnitude, enabling a reliable screening on electrolyte formulation at low temperature. More importantly,the model can be used to identify potential freezers with high efficiency, the capability of which emerged while learning to simple experimental data. Essentially, this work shows the power of combining experimental measurements with simulation tools, creating a self-reinforcing cycle that is much more capable than conventional one-shot MD simulations. Employing this method, we are able to conduct screening tasks for complex properties (such as phase-transition properties) while retaining the efficiency of classical MD. Such capability is well-evidencing for the AZIB electrolyte system in this work and is readily applicable to larger-scale screening problems for other molecular materials. Therefore, We believe these efforts address critical challenges in the design of AZIB electrolytes and pave the way for their broader application.

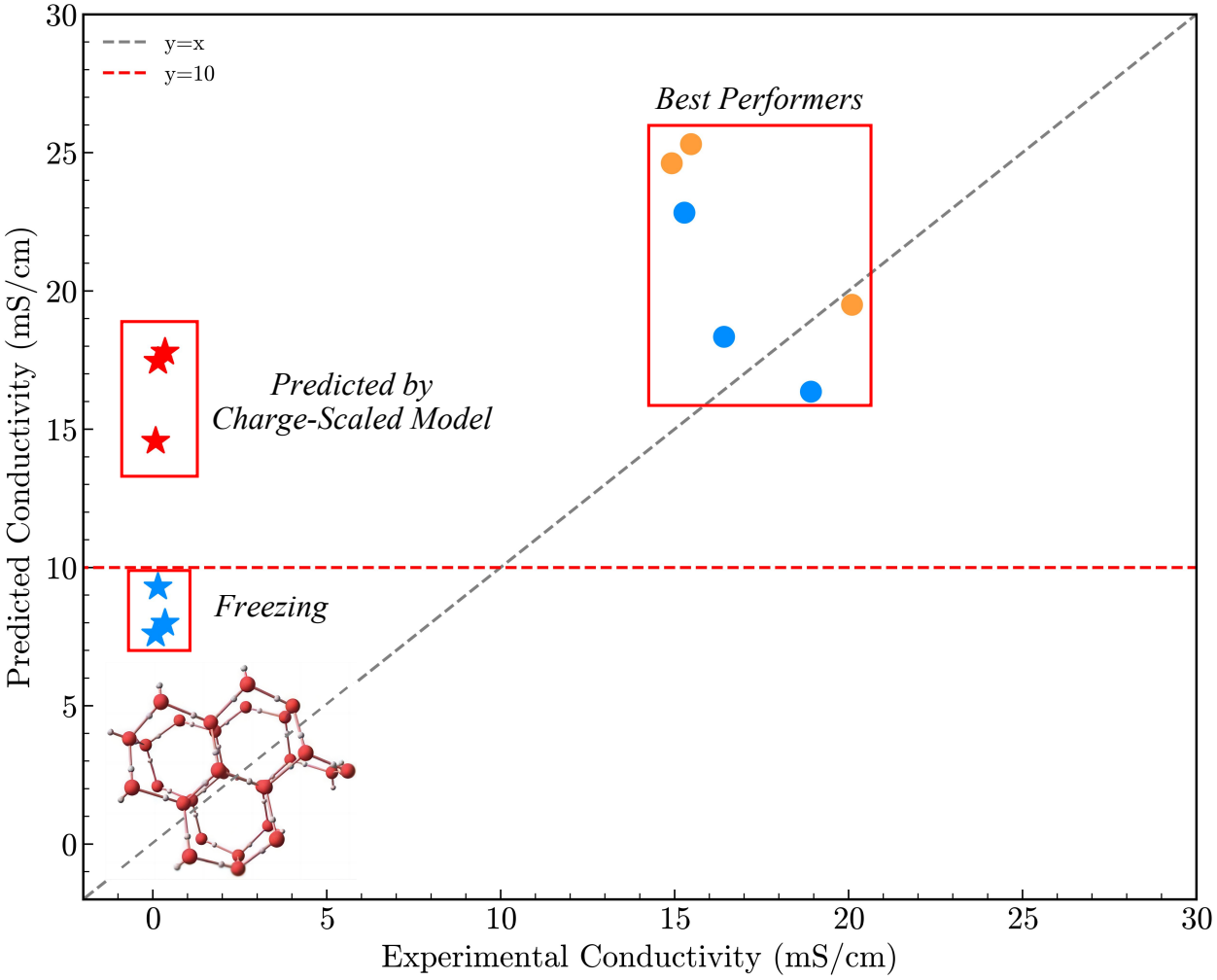

Figure 5: Exploration of new electrolyte formulations, predicted conductivities are plotted against experimental conductivities: best performers are labeled by dots and freezers are labeled by stars. Data points from the original dataset are in yellow, while newly explored data points are in blue. Red stars are the freezers computed using naive charge-scaled models.

Supporting Information Available

Experimental dataset; Experimental methods; Parameters of force field; Details of MD simulations; The comparison of different models; The correlation between temperature and scaling factor.

Author Contributions and Notes

W.F. and L.Z. are co-first authors and contributed equally to this work. The authors declare no competing financial interest.

Acknowledgement

The authors thank the National Natural Science of Foundation of China (Grant Number: 22473068) and Ministry of Science and Technology of the People´s Republic of China (National Key Research and Development Program of China, Project Number: 2022YFB2404502) for their financial supports to this work.

References

(1) High-throughput screening of halide solid-state electrolytes for all-solid-state Li-ion batteries through structural descriptor. *Journal of Alloys and Compounds* **2025**, *1010*, 177167, Publisher: Elsevier.

(2) Robotised screening and characterisation for accelerated discovery of novel Lithium-ion battery electrolytes: Building a platform and proof of principle studies. *Chemical Engineering Journal* **2023**, *455*, 140955, Publisher: Elsevier.

(3) Chen, X.; Liu, M.; Yin, S.; Gao, Y.-C.; Yao, N.; Zhang, Q. Uni-Electrolyte: An Artificial

Intelligence Platform for Designing Electrolyte Molecules for Rechargeable Batteries. 2024; http://arxiv.org/abs/2412.00498, arXiv:2412.00498 [cond-mat].

(4) Zhang, J.; Pagotto, J.; Duignan, T. T. Towards predictive design of electrolyte solutions by accelerating ab initio simulation with neural networks. *Journal of Materials Chemistry A* **2022**, *10*, 19560–19571, Publisher: The Royal Society of Chemistry.

(5) Chen, F.; O'Dell, L. A.; Pal, U.; Forsyth, M. In *Computational Design of Battery Materials*; Hanaor, D. A. H., Ed.; Springer International Publishing: Cham, 2024; pp 511–526.

(6) Challenges and Strategies for High-Energy Aqueous Electrolyte Rechargeable Batteries - Zhang - 2021 - Angewandte Chemie International Edition - Wiley Online Library. https://onlinelibrary.wiley.com/doi/full/10.1002/anie.202004433.

(7) Aqueous batteries as grid scale energy storage solutions. *Renewable and Sustainable Energy Reviews* **2017**, *68*, 1174–1182, Publisher: Pergamon.

(8) Kim, H.; Hong, J.; Park, K.-Y.; Kim, H.; Kim, S.-W.; Kang, K. Aqueous Rechargeable Li and Na Ion Batteries. *Chemical Reviews* **2014**, *114*, 11788–11827, Publisher: American Chemical Society.

(9) Recent Progress of Rechargeable Batteries Using Mild Aqueous Electrolytes - Huang - 2019 - Small Methods - Wiley Online Library. https://onlinelibrary.wiley.com/doi/abs/10.1002/smtd.201800272.

(10) Mongird, K.; Viswanathan, V. V.; Balducci, P. J.; Alam, M. J. E.; Fotedar, V.; Koritarov, V. S.; Hadjerioua, B. *Energy Storage Technology and Cost Characterization Report*; 2019.

(11) Recent Progress in Aqueous Lithium-Ion Batteries - Wang - 2012 - Advanced Energy

Materials - Wiley Online Library. https://onlinelibrary.wiley.com/doi/abs/10.1002/aenm.201200065.

(12) Doughty, D. H.; Butler, P. C.; Akhil, A. A.; Clark, N. H.; Boyes, J. D. Batteries for Large-Scale Stationary Electrical Energy Storage. *The Electrochemical Society Interface* **2010**, *19*, 49, Publisher: IOP Publishing.

(13) Suo, L.; Borodin, O.; Gao, T.; Olguin, M.; Ho, J.; Fan, X.; Luo, C.; Wang, C.; Xu, K. "Water-in-salt" electrolyte enables high-voltage aqueous lithium-ion chemistries. *Science* **2015**, *350*, 938–943, Publisher: American Association for the Advancement of Science.

(14) Design Strategies for Anti-Freeze Electrolytes in Aqueous Energy Storage Devices at Low Temperatures - You - Advanced Functional Materials - Wiley Online Library. https://onlinelibrary.wiley.com/doi/abs/10.1002/adfm.202403616.

(15) Han, J.; Mariani, A.; Passerini, S.; Varzi, A. A perspective on the role of anions in highly concentrated aqueous electrolytes. *Energy & Environmental Science* **2023**, *16*, 1480–1501, Publisher: Royal Society of Chemistry.

(16) Ji, D.; Kim, J. Trend of Developing Aqueous Liquid and Gel Electrolytes for Sustainable, Safe, and High-Performance Li-Ion Batteries. *Nano-Micro Letters* **2023**, *16*, 2.

(17) Electrolyte additive of sorbitol rendering aqueous zinc-ion batteries with dendrite-free behavior and good anti-freezing ability. *Chemical Engineering Journal* **2023**, *458*, 141392, Publisher: Elsevier.

(18) Wang, L.; Menakath, A.; Han, F.; Wang, Y.; Zavalij, P. Y.; Gaskell, K. J.; Borodin, O.; Iuga, D.; Brown, S. P.; Wang, C.; Xu, K.; Eichhorn, B. W. Identifying the components of the solid–electrolyte interphase in Li-ion batteries. *Nature Chemistry* **2019**, *11*, 789–796, Publisher: Nature Publishing Group.

(19) Modelling Bulk Electrolytes and Electrolyte Interfaces with Atomistic Machine Learning - Shao - 2021 - Batteries & Supercaps - Wiley Online Library. https://chemistry-europe.onlinelibrary.wiley.com/doi/full/10.1002/batt.202000262.

(20) Wang, J.; Olsson, S.; Wehmeyer, C.; Pérez, A.; Charron, N. E.; de Fabritiis, G.; Noé, F.; Clementi, C. Machine Learning of Coarse-Grained Molecular Dynamics Force Fields. *ACS Central Science* **2019**, *5*, 755–767, Publisher: American Chemical Society.

(21) Zhang, L.; Han, J.; Wang, H.; Car, R.; E, W. Deep Potential Molecular Dynamics: A Scalable Model with the Accuracy of Quantum Mechanics. *Physical Review Letters* **2018**, *120*, 143001, Publisher: American Physical Society.

(22) Gong, S.; Zhang, Y.; Mu, Z.; Pu, Z.; Wang, H.; Yu, Z.; Chen, M.; Zheng, T.; Wang, Z.; Chen, L.; Wu, X.; Shi, S.; Gao, W.; Yan, W.; Xiang, L. BAMBOO: a predictive and transferable machine learning force field framework for liquid electrolyte development. 2024; http://arxiv.org/abs/2404.07181, arXiv:2404.07181 [cond-mat, physics:physics].

(23) Kovács, D. P.; Moore, J. H.; Browning, N. J.; Batatia, I.; Horton, J. T.; Kapil, V.; Witt, W. C.; Magdău, I.-B.; Cole, D. J.; Csányi, G. MACE-OFF23: Transferable Machine Learning Force Fields for Organic Molecules. 2023; http://arxiv.org/abs/2312.15211, arXiv:2312.15211 [physics].

(24) Chen, J.; Yu, K. PhyNEO: A Neural-Network-Enhanced Physics-Driven Force Field Development Workflow for Bulk Organic Molecule and Polymer Simulations. *Journal of Chemical Theory and Computation* **2024**, *20*, 253–265, Publisher: American Chemical Society.

(25) Jorgensen, W. L.; Maxwell, D. S.; Tirado-Rives, J. Development and Testing of the OPLS All-Atom Force Field on Conformational Energetics and Properties of Organic

Liquids. *Journal of the American Chemical Society* **1996**, *118*, 11225–11236, Publisher: American Chemical Society.

(26) Jorgensen, W. L.; Tirado-Rives, J. Potential energy functions for atomic-level simulations of water and organic and biomolecular systems. *Proceedings of the National Academy of Sciences* **2005**, *102*, 6665–6670, Publisher: Proceedings of the National Academy of Sciences.

(27) Cornell, W. D.; Cieplak, P.; Bayly, C. I.; Gould, I. R.; Merz, K. M.; Ferguson, D. M.; Spellmeyer, D. C.; Fox, T.; Caldwell, J. W.; Kollman, P. A. A Second Generation Force Field for the Simulation of Proteins, Nucleic Acids, and Organic Molecules. 2002; `https://pubs.acs.org/doi/pdf/10.1021/ja00124a002`, Archive Location: world Publisher: American Chemical Society.

(28) Development and testing of a general amber force field - Wang - 2004 - Journal of Computational Chemistry - Wiley Online Library. `https://onlinelibrary.wiley.com/doi/abs/10.1002/jcc.20035`.

(29) Senior, A. W. et al. Improved protein structure prediction using potentials from deep learning. *Nature* **2020**, *577*, 706–710, Publisher: Nature Publishing Group.

(30) CHARMM: The biomolecular simulation program - Brooks - 2009 - Journal of Computational Chemistry - Wiley Online Library. `https://onlinelibrary.wiley.com/doi/abs/10.1002/jcc.21287`.

(31) Niu, H.; Yang, Y. I.; Parrinello, M. Temperature Dependence of Homogeneous Nucleation in Ice. *Physical Review Letters* **2019**, *122*, 245501, Publisher: American Physical Society.

(32) Trejos, V. M.; de Lucas, M.; Vega, C.; Blazquez, S.; Gámez, F. Further extension of the Madrid-2019 force field: Parametrization of nitrate (NO3) and ammonium (NH4+) ions. *The Journal of Chemical Physics* **2023**, *159*, 224501.

(33) Habibi, P.; Polat, H. M.; Blazquez, S.; Vega, C.; Dey, P.; Vlugt, T. J. H.; Moultos, O. A. Accurate Free Energies of Aqueous Electrolyte Solutions from Molecular Simulations with Non-polarizable Force Fields. *The Journal of Physical Chemistry Letters* **2024**, *15*, 4477–4485, Publisher: American Chemical Society.

(34) Le Breton, G.; Joly, L. Molecular modeling of aqueous electrolytes at interfaces: Effects of long-range dispersion forces and of ionic charge rescaling. *The Journal of Chemical Physics* **2020**, *152*, 241102.

(35) Doerr, S.; Majewski, M.; Pérez, A.; Krämer, A.; Clementi, C.; Noe, F.; Giorgino, T.; De Fabritiis, G. TorchMD: A Deep Learning Framework for Molecular Simulations. *Journal of Chemical Theory and Computation* **2021**, *17*, 2355–2363, Publisher: American Chemical Society.

(36) Schoenholz, S. S.; Cubuk, E. D. JAX, M.D. A framework for differentiable physics*. *Journal of Statistical Mechanics: Theory and Experiment* **2021**, *2021*, 124016, Publisher: IOP Publishing and SISSA.

(37) SPONGE: A GPU-Accelerated Molecular Dynamics Package with Enhanced Sampling and AI-Driven Algorithms - Huang - 2022 - Chinese Journal of Chemistry - Wiley Online Library. `https://onlinelibrary.wiley.com/doi/abs/10.1002/cjoc.202100456`.

(38) Wang, X.; Li, J.; Yang, L.; Chen, F.; Wang, Y.; Chang, J.; Chen, J.; Feng, W.; Zhang, L.; Yu, K. DMFF: An Open-Source Automatic Differentiable Platform for Molecular Force Field Development and Molecular Dynamics Simulation. *Journal of Chemical Theory and Computation* **2023**, *19*, 5897–5909, Publisher: American Chemical Society.

(39) Fröhlking, T.; Bernetti, M.; Calonaci, N.; Bussi, G. Toward empirical force fields that match experimental observables. *The Journal of Chemical Physics* **2020**, *152*, 230902.

(40) Norgaard, A. B.; Ferkinghoff-Borg, J.; Lindorff-Larsen, K. Experimental Parameterization of an Energy Function for the Simulation of Unfolded Proteins. *Biophysical Journal* **2008**, *94*, 182–192.

(41) Bottaro, S.; Lindorff-Larsen, K.; Best, R. B. Variational Optimization of an All-Atom Implicit Solvent Force Field To Match Explicit Solvent Simulation Data. *Journal of Chemical Theory and Computation* **2013**, *9*, 5641–5652, Publisher: American Chemical Society.

(42) Wang, L.-P.; Head-Gordon, T.; Ponder, J. W.; Ren, P.; Chodera, J. D.; Eastman, P. K.; Martinez, T. J.; Pande, V. S. Systematic Improvement of a Classical Molecular Model of Water. *The Journal of Physical Chemistry B* **2013**, *117*, 9956–9972, Publisher: American Chemical Society.

(43) Wang, L.-P.; Martinez, T. J.; Pande, V. S. Building Force Fields: An Automatic, Systematic, and Reproducible Approach. *The Journal of Physical Chemistry Letters* **2014**, *5*, 1885–1891, Publisher: American Chemical Society.

(44) Berendsen, H. J. C.; Grigera, J. R.; Straatsma, T. P. The missing term in effective pair potentials. 2002; `https://pubs.acs.org/doi/pdf/10.1021/j100308a038`, Archive Location: world Publisher: American Chemical Society.

(45) Haile, J. M. *Molecular Dynamics Simulation: Elementary Methods*, 1st ed.; John Wiley & Sons, Inc.: USA, 1992.

(46) Larsen, B. Studies in statistical mechanics of Coulombic systems. I. Equation of state for the restricted primitive model. *The Journal of Chemical Physics* **1976**, *65*, 3431–3438.

(47) Hansen, J.-P.; McDonald, I. R. *Theory of Simple Liquids: with Applications to Soft Matter*; Academic Press, 2013; Google-Books-ID: pbJfOUqZVSgC.

(48) Allen, M. P.; Tildesley, D. J. *Computer Simulation of Liquids*; Oxford University Press, 2017; Google-Books-ID: WFExDwAAQBAJ.

(49) Vanommeslaeghe, K.; MacKerell, A. D. J. Automation of the CHARMM General Force Field (CGenFF) I: Bond Perception and Atom Typing. *Journal of Chemical Information and Modeling* **2012**, *52*, 3144–3154, Publisher: American Chemical Society.

(50) Molecular Dynamics Simulations of Ionic Liquids and Electrolytes Using Polarizable Force Fields | Chemical Reviews. `https://pubs.acs.org/doi/full/10.1021/acs.chemrev.8b00763`.

(51) Kostal, V.; Jungwirth, P.; Martinez-Seara, H. Nonaqueous Ion Pairing Exemplifies the Case for Including Electronic Polarization in Molecular Dynamics Simulations. *The Journal of Physical Chemistry Letters* **2023**, *14*, 8691–8696, Publisher: American Chemical Society.

(52) Cui, K.; Yethiraj, A.; Schmidt, J. R. Influence of Charge Scaling on the Solvation Properties of Ionic Liquid Solutions. *The Journal of Physical Chemistry B* **2019**, *123*, 9222–9229, Publisher: American Chemical Society.

(53) Duboué-Dijon, E.; Javanainen, M.; Delcroix, P.; Jungwirth, P.; Martinez-Seara, H. A practical guide to biologically relevant molecular simulations with charge scaling for electronic polarization. *The Journal of Chemical Physics* **2020**, *153*, 050901.

(54) Thaler, S.; Zavadlav, J. Learning neural network potentials from experimental data via Differentiable Trajectory Reweighting. *Nature Communications* **2021**, *12*, 6884, Publisher: Nature Publishing Group.

(55) Lide, D. R., Ed. *CRC Handbook of Chemistry and Physics, 87th Edition*, 87 ed.; CRC Press: Boca Raton, Fla., 2006.

(56) Wang, J.; Hou, T. Application of Molecular Dynamics Simulations in Molecular Property Prediction. 1. Density and Heat of Vaporization. *Journal of Chemical Theory and Computation* **2011**, *7*, 2151–2165, Publisher: American Chemical Society.

(57) Molecular dynamics study of conductivity of ionic liquids: The Kohlrausch law. *Journal of Molecular Liquids* **2007**, *134*, 29–33, Publisher: Elsevier.

(58) Schröder, C.; Haberler, M.; Steinhauser, O. On the computation and contribution of conductivity in molecular ionic liquids. *The Journal of Chemical Physics* **2008**, *128*, 134501.

(59) Blazquez, S.; Abascal, J. L. F.; Lagerweij, J.; Habibi, P.; Dey, P.; Vlugt, T. J. H.; Moultos, O. A.; Vega, C. Computation of Electrical Conductivities of Aqueous Electrolyte Solutions: Two Surfaces, One Property. *Journal of Chemical Theory and Computation* **2023**, *19*, 5380–5393, Publisher: American Chemical Society.

(60) Schröder, C.; Haberler, M.; Steinhauser, O. On the computation and contribution of conductivity in molecular ionic liquids. *The Journal of Chemical Physics* **2008**, *128*, 134501.

(61) Molecular dynamics study of conductivity of ionic liquids: The Kohlrausch law. *Journal of Molecular Liquids* **2007**, *134*, 29–33, Publisher: Elsevier.

(62) Calculations of shear viscosity, electric conductivity and diffusion coefficients of aqueous sodium perchlorate solutions from molecular dynamics simulations. *Computational and Theoretical Chemistry* **2016**, *1090*, 52–57, Publisher: Elsevier.

(63) Yao, N.; Chen, X.; Fu, Z.-H.; Zhang, Q. Applying Classical, Ab Initio, and Machine-Learning Molecular Dynamics Simulations to the Liquid Electrolyte for Rechargeable Batteries. *Chemical Reviews* **2022**, *122*, 10970–11021, Publisher: American Chemical Society.

(64) Feng, G.; Chen, M.; Bi, S.; Goodwin, Z. A.; Postnikov, E. B.; Brilliantov, N.; Urbakh, M.; Kornyshev, A. A. Free and Bound States of Ions in Ionic Liquids, Conductivity, and Underscreening Paradox. *Physical Review X* **2019**, *9*, 021024, Publisher: American Physical Society.

(65) Temperature dependence of the transport coefficients of ions from molecular dynamics simulations. *Chemical Physics Letters* **2005**, *408*, 84–88, Publisher: North-Holland.

(66) An overview of the Amber biomolecular simulation package - Salomon-Ferrer - 2013 - WIREs Computational Molecular Science - Wiley Online Library. `https://wires.onlinelibrary.wiley.com/doi/abs/10.1002/wcms.1121`.

(67) Case, D. A.; Cheatham III, T. E.; Darden, T.; Gohlke, H.; Luo, R.; Merz Jr., K. M.; Onufriev, A.; Simmerling, C.; Wang, B.; Woods, R. J. The Amber biomolecular simulation programs. *Journal of Computational Chemistry* **2005**, *26*, 1668–1688, _eprint: https://onlinelibrary.wiley.com/doi/pdf/10.1002/jcc.20290.

(68) PACKMOL: A package for building initial configurations for molecular dynamics simulations - Martínez - 2009 - Journal of Computational Chemistry - Wiley Online Library. `https://onlinelibrary.wiley.com/doi/full/10.1002/jcc.21224`.

(69) Eastman, P.; Pande, V. OpenMM: A Hardware-Independent Framework for Molecular Simulations. *Computing in Science & Engineering* **2010**, *12*, 34–39, Conference Name: Computing in Science & Engineering.

(70) Eastman, P.; Swails, J.; Chodera, J. D.; McGibbon, R. T.; Zhao, Y.; Beauchamp, K. A.; Wang, L.-P.; Simmonett, A. C.; Harrigan, M. P.; Stern, C. D.; Wiewiora, R. P.; Brooks, B. R.; Pande, V. S. OpenMM 7: Rapid development of high performance algorithms for molecular dynamics. *PLOS Computational Biology* **2017**, *13*, e1005659, Publisher: Public Library of Science.

(71) Duboué-Dijon, E.; Javanainen, M.; Delcroix, P.; Jungwirth, P.; Martinez-Seara, H. A practical guide to biologically relevant molecular simulations with charge scaling for electronic polarization. *The Journal of Chemical Physics* **2020**, *153*, 050901.

(72) Kirby, B. J.; Jungwirth, P. Charge Scaling Manifesto: A Way of Reconciling the Inherently Macroscopic and Microscopic Natures of Molecular Simulations. *The Journal of Physical Chemistry Letters* **2019**, *10*, 7531–7536, Publisher: American Chemical Society.